Pergamon

Int. J. Solids Structures Vol. 34, No. 24, pp. 3099–3118, 1997

0020-7683/97 $17.00 + .00

PII: S0020-7683(96)00174-6

AN ANALYSIS OF THE INFLUENCE OF THE PRESSURIZATION RATE ON THE BOREHOLE BREAKDOWN PRESSURE

D. GARAGASH and E. DETOURNAY†
Department of Civil Engineering, University of Minnesota, 500 Pillsbury Dr. S. E., Minneapolis, MN 55455-0220, U.S.A.

(*Received* 20 *March* 1996; *in revised form* 9 *August* 1996)

Abstract—This paper investigates the dependence of breakdown pressure, the critical pressure at which tensile failure of the rock is initiated by injecting fluid in a borehole, on the rate of pressurization. The mathematical model explicitly accounts for the existence of micro-cracks at the borehole wall that trigger the failure process. Breakdown, in this context, occurs when the stress intensity factor of a critically oriented micro-crack reaches the rock toughness. The model is presently restricted to low-permeability/low-porosity rocks. By considering one-dimensional lubrication flow in the crack coupled with the non-local elastic response of the crack, the evolution of the net pressure, crack opening and stress intensity factor is obtained as functions of the pressurization rate. The relation between breakdown pressure and pressurization rate in the case of zero initial net pressure is shown to be controlled by only one dimensionless number: the ratio between the initial width of the unstressed micro-crack and the induced elastic opening at failure. It is further shown that (i) the fluid pressure in the early stages of the pressurization history drops in the crack and that cavitation can occur, and (ii) local back-flow in the crack takes place. The dependence of breakdown pressure, p_b, on the pressurization rate, A, is determined as well as the range of A, where p_b varies significantly. The lower and pseudo upper bounds of this range of pressurization rate correspond to limiting regimes of slow and pseudo fast pressurization. © 1997 Elsevier Science Ltd.

NOMENCLATURE

a	borehole radius
p	fluid pressure
p_o	initial fluid pressure
p_w	borehole pressure
t	time
t_*	characteristic time
x	position
w	crack width
w_o	initial width at crack inlet
w_*	characteristic crack width
A	pressurization rate
E'	plane strain elastic modulus
T	tensile strength
K_{Ic}	toughness
P_o	far-field mean pressure
S_o	far-field stress deviator
λ	crack length
μ	fluid viscosity
σ	crack loading, according to the Lamé solution
τ	dimensionless time
ξ	dimensionless space coordinate
Π	dimensionless net crack loading
$\langle\Pi\rangle$	dimensionless stress intensity factor
Ω	dimensionless crack width
Ω_o	dimensionless initial crack width at the inlet
Ω_e	dimensionless elastically induced crack width ($\Omega = \Omega_o + \Omega_e$)
γ	dimensionless pressurization rate

† Author to whom correspondence should be addressed.

INTRODUCTION

The breakdown pressure, p_b, the critical pressure at which tensile failure ("breakdown") is initiated at a borehole wall by fluid injection, is a crucial parameter in hydraulic fracturing tests carried out to determine the *in-situ* stress field in a rock mass. This method consists in hydraulically pressurizing an interval of a vertical borehole to initiate and propagate two symmetric vertical fractures in the direction perpendicular to the minimum compressive *in-situ* stress (Haimson (1978)). The pressure-time record is then interpreted to provide estimates of the *in-situ* stress. In particular, the peak pressure or breakdown pressure is indicative of the initiation of a fracture at the borehole wall.

Several breakdown criteria (Hubbert and Willis (1957), Haimson and Fairhurst (1967)) have been proposed to relate the value of p_b to the far-field stress and rock properties. However, these criteria predict the breakdown pressure p_b to be independent of the pressurization rate A, despite strong experimental evidence indicating that p_b does vary with A, i.e., $p_b = p_b(A)$ (Haimson and Zhao (1991), Schmitt and Zoback (1992), (1993)). Recent studies (Detournay and Cheng (1992), Detournay and Carbonell (1994)) actually suggest that the classical breakdown criteria correspond to the slow and fast asymptotic regimes of pressurization rate, under the limiting condition that the length λ of pre-existing defects (which trigger the tensile failure process) is small compared to the borehole radius a. Thus, the task of determining this relation and the bounds of the range of A, where the breakdown pressure varies significantly with the pressurization rate, appears to be important for interpreting results of *in-situ* hydraulic fracturing stress tests.

An attempt to model the dependence of the breakdown pressure on the pressurization rate in permeable rock was previously made by introducing a length scale λ to characterize the failure process and by assuming that breakdown takes place when the Terzaghi effective stress, averaged over λ, reaches a critical value (Detournay and Cheng (1992)). Threshold values of the pressurization rate, A_l and A_u, for slow and fast asymptotic regimes, respectively, were then obtained by considering the evolution of the pore-pressure perturbation near the permeable boundary of the borehole. The values A_l and A_u calculated for typical sets of material parameters are, however, much higher than those observed in experiments, and their ratio is also two to three orders of magnitude higher than the experimental values. Finally, such a model is not really appropriate for low-permeability rocks, where pore-pressure diffusion in the rock matrix is negligible over the duration of the experiment.

Thus, in order to improve the prediction of bounds A_l and A_u and to incorporate the case of low-permeability rock, we explicitly take into account the existence of micro-cracks at the boundary of the borehole and fluid flow in these micro-cracks to calculate the conditions leading to failure. The micro-cracks could either be material defects (initially present in the rock) or be the result of stress relief following drilling of the hole. The defects are defined by the length λ and initial opening (at zero net pressure) w_o. Both values are assumed to be characteristics of the *in-situ* rock. We will narrow our investigation to the case when leakage from the micro-crack is negligible (which is a valid approximation for low permeability rocks).

The objectives of this paper are two-fold: firstly to investigate features of the net pressure evolution in the micro-crack during pressurization of the borehole; secondly to find the asymptotic slow and fast pressurization regimes and their dependence upon the set of dimensionless parameters which characterize the geometry of the crack, the elastic properties of the rock and the initial loading.

PROBLEM DESCRIPTION AND GOVERNING EQUATIONS

Problem definition

Consider a borehole with radius a in an elastic domain with length scale L under internal fluid pressure p_w and far-field loading characterized by isotropic and deviatoric components, P_o and S_o, respectively. Consider also a critically oriented crack of length λ at the edge of the borehole, which is aligned with the far-field maximum compressive stress

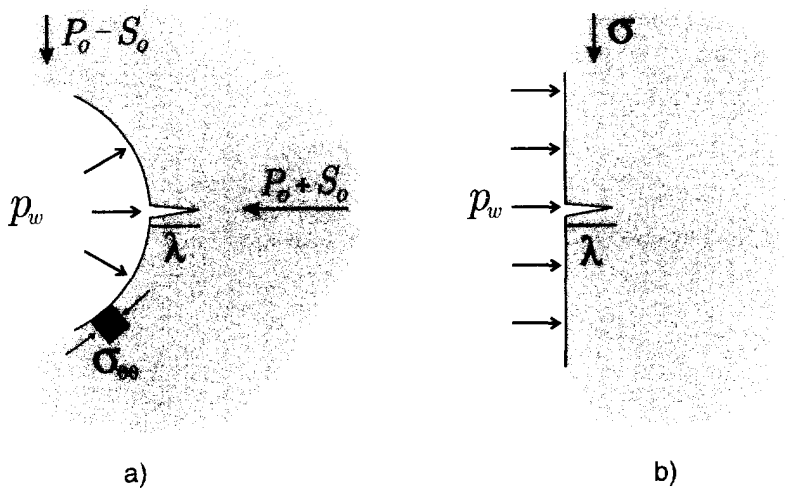

Fig. 1. Problem description and one-dimensional approximation by an edge-crack.

direction (see Fig. 1a). Assuming that $L \gg a \gg \lambda$, the defect can actually be treated as an edge crack of a half-plane subjected to a far-field loading σ in the direction perpendicular to the crack (see Fig. 1b and Fig. 2). With this assumption, the borehole radius a is effectively removed as a parameter controlling this problem. Making this assumption we exclude any borehole size effect on the solution of the problem. The loading σ then corresponds to the hoop stress that exists at the hole boundary in the absence of a crack; according to Lamé solution,

$$\sigma(t) = 2P_o - 4S_o - p_w(t). \tag{1}$$

We assume that the fluid pressure p in the crack is initially equilibrated, and therefore equal to the initial pressure in the borehole $p_w(0) = p_o$. Furthermore, we consider here the case of zero initial net crack loading—i.e., $p(0) - \sigma(0) = 0$. (If the initial net loading on the crack is negative, the crack is closed and the system evolution is trivial until $p - \sigma = 0$.)

Governing equations

For typical values of parameters characterizing the crack geometry and the elastic properties of the rock and the fluid, it can be shown that the fluid compressibility has no effect in this problem (see Appendix A). Hence, the governing equation for the flow inside

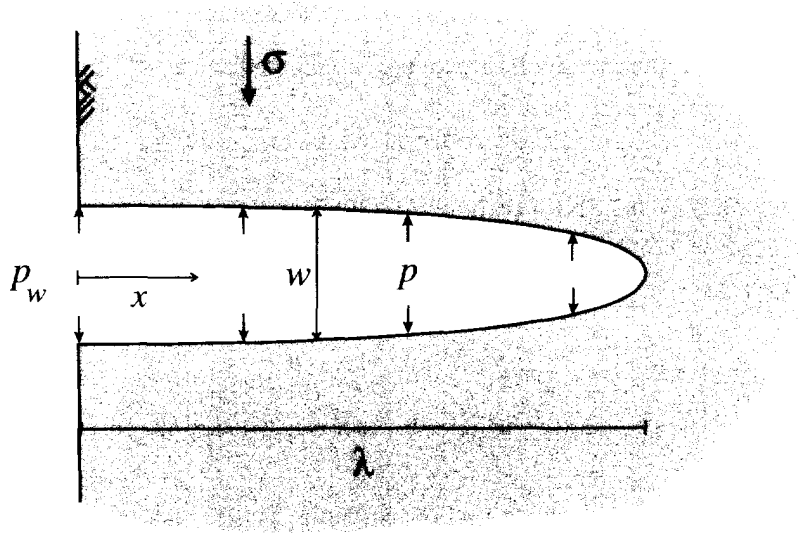

Fig. 2. Description of the edge crack problem.

the crack is given by the lubrication equation for incompressible fluid, or Reynolds equation (Shapiro (1954))

$$\frac{1}{12\mu}\frac{\partial}{\partial x}\left(w^3\frac{\partial p}{\partial x}\right)=\frac{\partial w}{\partial t} \tag{2}$$

which is obtained by combining the fluid mass balance equation

$$\frac{\partial w}{\partial t}=-\frac{\partial q}{\partial x} \tag{3}$$

with Poiseuille law

$$q=-\frac{w^3}{12\mu}\frac{\partial p}{\partial x}. \tag{4}$$

In the above, q is the volumetric flow rate, μ the fluid viscosity, p the fluid pressure, and w the crack opening.

The other governing equation is an elasticity relation between the crack opening w and the net crack loading $(p-\sigma)$. This relation is an integral equation which can be expressed as (Paris *et al.* (1976))

$$w=w_o\sqrt{1-\left(\frac{x}{\lambda}\right)^2}+\frac{2}{\lambda E'}\int_x^\lambda\left(\int_0^\eta[p(\zeta,t)-\sigma(t)]m(\zeta;\eta)\,\mathrm{d}\zeta\right)m(x;\eta)\eta\,\mathrm{d}\eta \tag{5}$$

where m is the Bueckner-Rice (1970, 1972) weight function, and E' is the so-called plane strain modulus, which is related to Young's modulus E and Poisson ratio ν by $E'=E/(1-\nu^2)$. Note that an initial opening distribution (equal to w_o at the crack inlet) at zero net crack loading has been added in (5) to the elastically induced crack width. Both the initial opening w_o and the length λ of the micro-crack are assumed to be material parameters.

The weight function m for an edge crack can be written as

$$m(x;\lambda)=2\left(\frac{\lambda}{\pi}\right)^{1/2}\frac{f(x/\lambda)}{(\lambda^2-x^2)^{1/2}} \tag{6}$$

where we adopt the approximation for $f(\xi)$ proposed by Nilson and Proffer (1984)

$$f(\xi)=\chi_1-\chi_2\xi \tag{7}$$

with $\chi_1=1.3$ and $\chi_2=0.3$. (Note that, for a Griffith crack, $\chi_1=1$ and $\chi_2=0$ or $f(\xi)=1$.)

Initial-boundary conditions are as follows

$$\begin{aligned} p&=p_o \quad \text{at } t=0\\ p&=p_w(t) \quad \text{at } x=0\\ w^3\frac{\partial p}{\partial x}&=0 \quad \text{at } x=\lambda \end{aligned} \tag{8}$$

where the last equation prescribes a no-flow condition at the crack tip. Here we consider specifically the case where the borehole pressure varies linearly in time,

$$p_w = p_o + At \tag{9}$$

where A is the constant pressurization rate.

It is interesting to point out that the no-flow condition at the crack tip does not necessarily imply that the pressure gradient vanishes at $x = \lambda$, since the crack width is equal to zero at that point. An expression for the pressure gradient at $x = \lambda$ can actually be derived from consideration of the crack tip asymptotics. First note that the fracture width near the tip (i.e., $1 - x/\lambda \ll 1$) is given by (Rice (1968))

$$w = \alpha(t)[2\lambda(\lambda - x)]^{1/2} \quad \text{with } \lambda - x \ll \lambda \tag{10}$$

where the dimensionless coefficient $\alpha(t)$ is

$$\alpha(t) = \left[\frac{w_o}{\lambda} + \frac{4K_I(t)}{(\pi\lambda)^{1/2}E'}\right].$$

Integrating the continuity eqn (2) over a small interval adjacent to the tip and making use of (10) yields

$$q = \frac{8K_I}{3E'}\left(\frac{2}{\pi}\right)^{1/2}(\lambda - x)^{3/2} \quad \text{with } \lambda - x \ll \lambda. \tag{11}$$

(Note that the dependance on time of these asymptotic fields is through the stress intensity factor K_I.) Finally, by comparing (4) and (11), we deduce that the pressure gradient at the crack tip is finite and given by

$$\frac{\partial p}{\partial x} = -\frac{16\mu\dot{K}_I(t)}{\sqrt{\pi\lambda^3}E'\alpha^3(t)} \quad \text{at } x = \lambda \tag{12}$$

where $\dot{K}_I$ denotes the rate of change of the stress intensity factor.

Condition for breakdown

The condition at which breakdown will occur is of concern in this paper. At breakdown, the stress intensity factor K_I reaches the critical value K_{Ic} (the rock toughness) and the crack starts to propagate. The stress intensity factor is given by the following integral relation in terms of the Bueckner-Rice weight function m (Bueckner (1970), Rice (1972))

$$K_I(t) = \int_0^\lambda [p(x,t) - \sigma(t)]m(x;\lambda)\,\mathrm{d}x. \tag{13}$$

Using expression (6) for m, the breakdown condition, $K_I = K_{Ic}$, can be conveniently rewritten as

$$\frac{2}{\chi\pi}\int_0^\lambda \frac{[p(x,t) - \sigma(t)]f(x/\lambda)}{\sqrt{\lambda^2 - x^2}}\mathrm{d}x = T \tag{14}$$

where the "tensile strength" of the rock T and the number χ are given by

$$T = \frac{K_{Ic}}{\chi\sqrt{\pi\lambda}}, \quad \chi = \frac{2}{\pi}\int_0^\lambda \frac{f(x/\lambda)}{\sqrt{\lambda^2 - x^2}}\mathrm{d}x \simeq 1.11. \tag{15}$$

If the net crack loading is uniform—i.e., $p(x,t) - \sigma(t) = \sigma_*(t)$—the breakdown condition

simply corresponds to $\sigma_* = T$. Under conditions of "slow" pressurization, for example, the fluid pressure in the crack is virtually the same as the pressure in the borehole—i.e., $p(x, t) = p_w(t)$; hence, the breakdown condition (14) simply becomes

$$p_b - p_o = \frac{T}{2} \tag{16}$$

where p_b is the breakdown pressure. This is indeed the criterion proposed by Haimson and Fairhurst (1967). On the other hand, if the fluid pressure in the crack is the same as the initial pressure—i.e., $p(x, t) = p_o$ (assuming that such a state can exist)—then the breakdown pressure is deduced from (14) to be

$$p_b - p_o = T. \tag{17}$$

The above criterion is formally equivalent to the Hubbert-Willis breakdown condition (1957).

EVOLUTION OF CRACK OPENING AND FLUID PRESSURE

Dimensional considerations

The solution for the given initial-boundary value problem (2)–(9) depends on a set of 6 parameters: the elastic modulus of the rock E', the two lengthscales characterizing the micro-crack geometry, λ and w_o, the rock "tensile strength" T (which depends on the crack length λ), the fluid viscosity μ, and the rate of pressurization A. Since the initial net crack loading is assumed to be zero (i.e., $p_o - \sigma(0) = 2P_o - 4S_o - 2p_o = 0$), none of the loading parameters P_o, S_o and p_o directly influences the solution. Furthermore, λ and E' appear in the elasticity eqn (5) only through the ratio λ/E', once the double integral in this equation has been made dimensionless. Hence, according to dimensional analysis, two numbers are governing the breakdown process. Here, we chose these two numbers as a dimensionless initial width at the crack inlet Ω_o and a dimensionless rate of pressurization γ respectively defined as

$$\Omega_o = \frac{w_o}{w_*} \tag{18}$$

$$\gamma = \frac{At_*}{T} \tag{19}$$

where w_* is a measure of the elastically induced crack opening at breakdown†

$$w_* = \frac{\lambda T}{E'} \tag{20}$$

where t_* is the timescale

† The exact expression for the opening at the crack mouth at breakdown (i.e., $K_I = K_{Ic}$), under condition of uniform fluid pressure, is given by

$$w = w_o + \frac{8}{\pi}\chi_1\left(\chi_1\frac{\pi}{2} - \chi_2\right)w_* \quad \text{at } \xi = 0 \quad \text{if } (p - \sigma) = T$$

where the coefficient of proportionality in front of w_* is equal to 4 for Griffith crack and to approximately 5.767 for the edge crack.

$$t_* = \frac{12\mu E'^2}{T^3}. \tag{21}$$

This timescale can be interpreted as a measure of the time required to equilibrate a fluid pressure perturbation at pressure close to breakdown, when $\Omega_o \ll 1$. Thus the number Ω_o is proportional to the ratio of the initial crack opening and the elastically induced opening at breakdown, while γ represents the ratio of the characteristic time to a measure of the time required to reach breakdown.

Finally, we introduce the following dimensionless variables and field quantities: the position variable $\xi = x/\lambda$ $(0 \leqslant \xi \leqslant 1)$, the time $\tau = t/t_*$ $(t \geqslant 0)$, the net crack loading $\Pi(\xi, \tau) = (p-\sigma)/T$, and the crack width $\Omega(\xi, \tau) = w/w_*$.

The fact that the tensile strength T only enters in the list of parameters through the breakdown condition (14) (i.e., the evolution of the crack opening w and net pressure $p-\sigma$ does not depend on T) has some implications on the dependance of these functions on the parameters γ and Ω_o. Indeed, without first considering the breakdown condition, we can deduce from the Reynolds (2) and elasticity eqn (5), together with the initial/boundary conditions that

$$\begin{aligned} \Pi' &= \Pi'(\xi, \tau'; \gamma') \\ \Omega' &= \Omega'(\xi, \tau'; \gamma') \end{aligned} \tag{22}$$

where the new dimensionless quantities (denoted by a prime) are defined as

$$\Pi' = \frac{\lambda(p-\sigma)}{w_o E'}, \quad \Omega' = \frac{w}{w_o}, \quad \tau' = \frac{tE'w_o^3}{12\mu\lambda^3}, \quad \gamma' = \frac{12\mu A\lambda^4}{E'^2 w_o^4}. \tag{23}$$

(Note that τ' is the time scaled by $t_{**} = 12\mu\lambda^3/w_o^3 E'$, which can be interpreted as the characteristic time associated with equilibration of a fluid pressure perturbation in the crack at the initial opening w_o.) It can readily be established that the primed and unprimed quantities are related as follows

$$\Pi' = \Omega_o^{-1}\Pi, \quad \Omega' = \Omega_o^{-1}\Omega, \quad \tau' = \Omega_o^3\tau, \quad \gamma' = \Omega_o^{-4}\gamma \tag{24}$$

from which we conclude that

$$\begin{aligned} \Pi(\xi, \tau; \gamma, \Omega_o) &= \Omega_o \Pi'(\xi, \Omega_o^3\tau; \Omega_o^{-4}\gamma) \\ \Omega(\xi, \tau; \gamma, \Omega_o) &= \Omega_o \Omega'(\xi, \Omega_o^3\tau; \Omega_o^{-4}\gamma). \end{aligned} \tag{25}$$

The main implication of the above relationship is that once the two functions Π and Ω have been determined for a particular value of Ω_o (for $0 \leqslant \xi \leqslant 1$, $0 \leqslant \tau < \infty$, $0 < \gamma < \infty$), they can be computed for any other values of Ω_o through simple scaling of Π, Ω, τ, and γ.

Dimensionless form of the governing equations

The solution of the original initial-boundary value problem (2), (5), (8), (9) is equivalent to solving the following set of coupled non-linear integro-differential equations for $\Pi(\xi, \tau)$ and $\Omega(\xi, \tau)$

$$\frac{\partial \Omega}{\partial \tau} = \frac{\partial}{\partial \xi}\left(\Omega^3 \frac{\partial \Pi}{\partial \xi}\right) \tag{26}$$

$$\Omega = \Omega_0 \sqrt{1-\xi^2} + \frac{8}{\pi}\int_\xi^1 \left[\int_0^\eta \frac{\Pi f(\zeta/\eta)\,\mathrm{d}\zeta}{\sqrt{\eta^2-\zeta^2}}\right] \frac{f(\xi/\eta)\eta\,\mathrm{d}\eta}{\sqrt{\eta^2-\xi^2}} \tag{27}$$

subjected to initial and boundary conditions

$$\begin{aligned} \Pi &= 0 \quad \text{at } \tau = 0 \\ \Pi &= 2\gamma\tau \quad \text{at } \xi = 0 \\ \Omega^3 \frac{\partial \Pi}{\partial \xi} &= 0 \quad \text{at } \xi = 1. \end{aligned} \tag{28}$$

Note that the expression (12) for the pressure gradient at the tip translates into

$$\frac{\partial \Pi}{\partial \xi} = -\frac{4\chi}{3(\Omega_o + 4\chi\langle\Pi\rangle)^3}\frac{\mathrm{d}\langle\Pi\rangle}{\mathrm{d}t} \quad \text{at } \xi = 1 \tag{29}$$

where $\langle\Pi\rangle(\tau)$ is a particular weighted spatial average of the net crack loading

$$\langle\Pi\rangle \equiv \frac{2}{\pi\chi}\int_0^1 \frac{\Pi f(\xi)}{\sqrt{1-\xi^2}}\mathrm{d}\xi. \tag{30}$$

Actually, $\langle\Pi\rangle$ represents a dimensionless stress intensity factor, since the breakdown condition (14) can simply be expressed as

$$\langle\Pi\rangle = 1. \tag{31}$$

Evolution of fluid pressure and crack opening

Evolution in time of the net pressure field $\Pi(\xi,\tau)$ and crack opening $\Omega(\xi,\tau)$ is determined by solving numerically the initial boundary value problem defined by the system of coupled eqns (26) and (27) together with the conditions (28). The numerical procedure is based on the method of lines (Liskovets (1965), Nilson and Griffiths (1983)). This method approximates the set of eqns (26) and (27) by a coupled system of ordinary differential equations for the values of the net pressure at the grid points over the space interval representing the crack. Details of the numerical method are given in Appendix B.

The main features of the system response to a linear increase of the pressure at the boundary are illustrated in Figs 3–9, with the calculations performed for $\Omega_o = 2$, $\gamma = 4$,

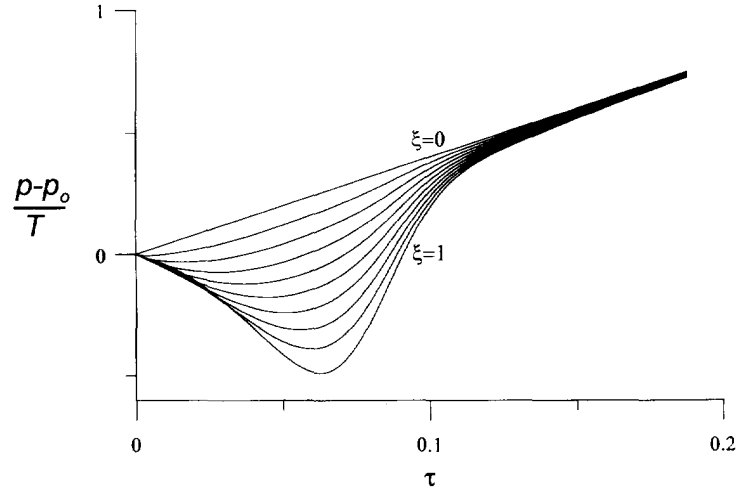

Fig. 3. Fluid pressure evolution with time along the crack from the inlet, $\xi = 0$, to the tip, $\xi = 1$.

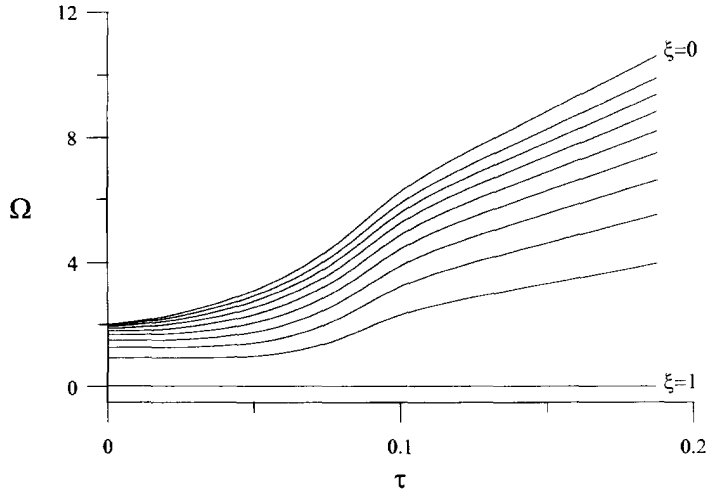

Fig. 4. Crack opening evolution with time along the crack from the inlet, $\xi = 0$, to the tip, $\xi = 1$.

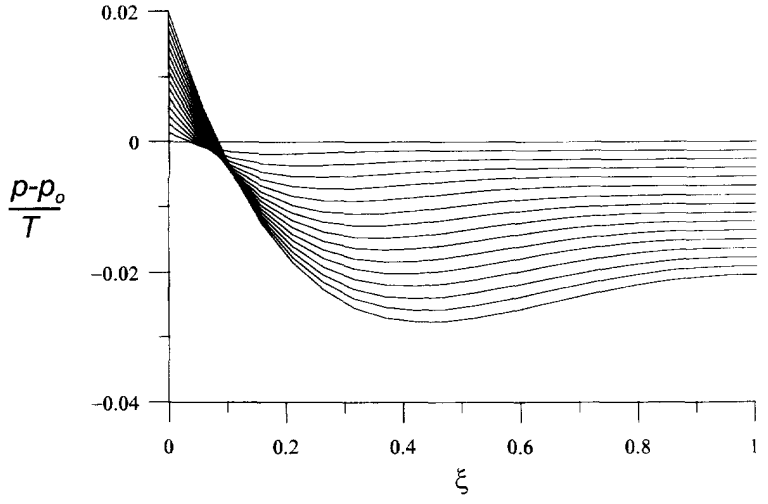

Fig. 5. Distribution of fluid pressure along the crack for early times.

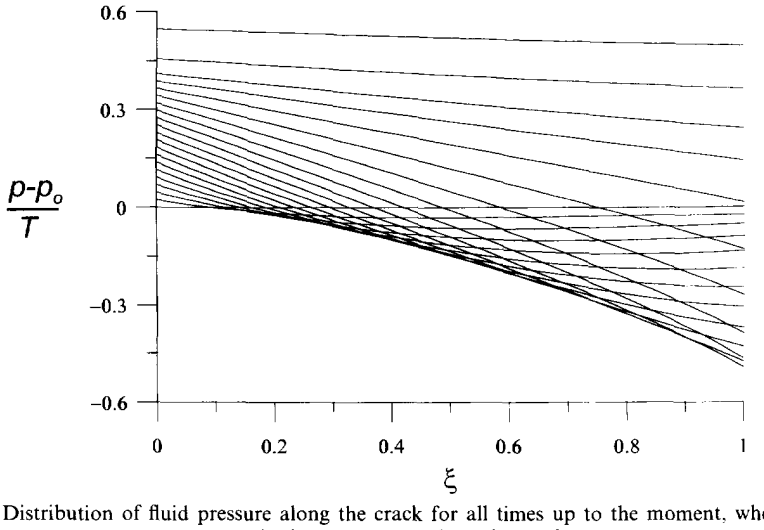

Fig. 6. Distribution of fluid pressure along the crack for all times up to the moment, when the pressure is almost constant along the crack.

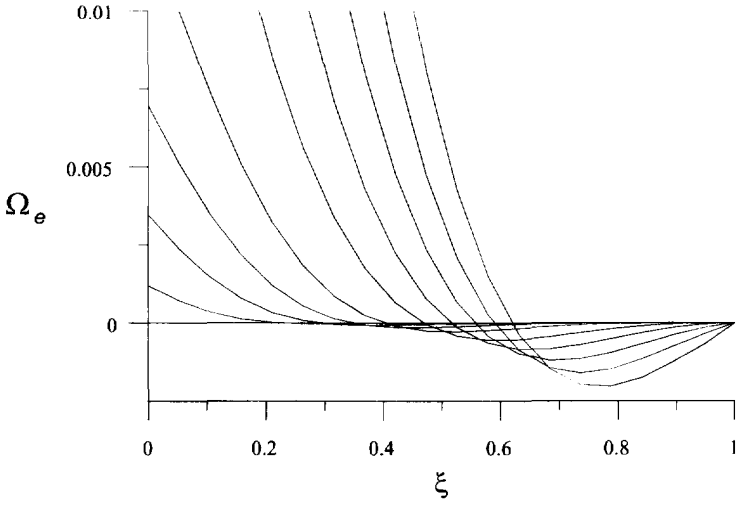

Fig. 7. Elastically induced crack opening plotted along the crack for early times.

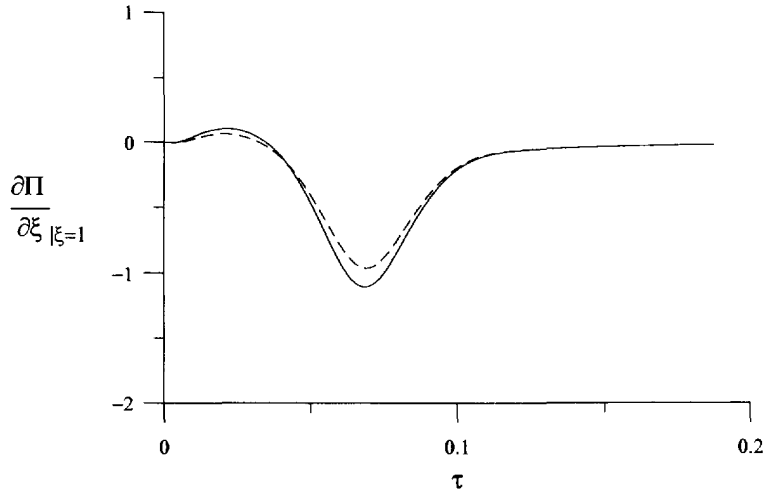

Fig. 8. Pressure gradient at the tip of the crack vs time: solid curve obtained by finite difference and dashed curve using the estimate of the stress intensity factor.

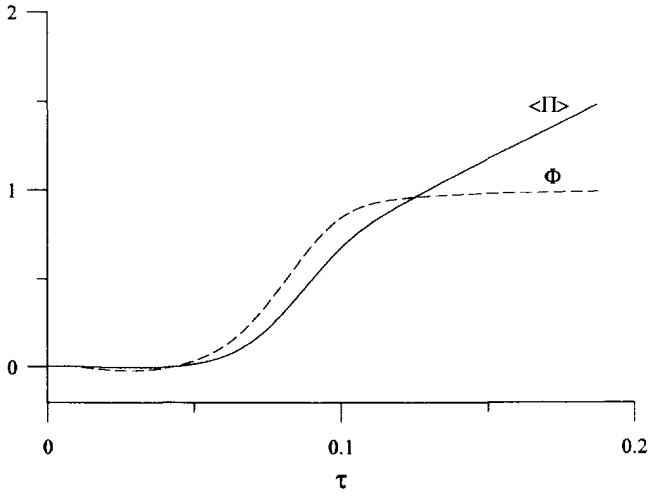

Fig. 9. Evolution of the influence function Φ and stress intensity factor $\langle \Pi \rangle$ with time.

using 20 grid points equally spaced along the crack. It is worthwhile to mention that the results produced with 10 grid points are practically the same as those obtained with 20 grid points.

Consider first Figs 3 and 4 showing the evolution of the fluid pressure variation $(p-p_o)/T$ and scaled opening Ω at various positions $\xi = 0, 1/9, \ldots, 1$ along the crack. The main features of Fig. 3 are the drop of pressure in the crack at early times and the gradual increase of the pressure towards the prescribed boundary pressure at large time, after attaining a minimum. This early time drop of the fluid pressure in the crack is directly attributable to the "non-local" character of the crack deformation, which is embodied in the integral relationship (27) between the opening Ω and the net pressure Π. (Similar behaviors—sometimes called "negative initial pressure effect" or "reverse pressure effect"—have been reported in physical pumping tests in jointed rock masses (Pine (1986)) and in numerical simulations of such tests (Cundall (1991)).) Note that it is implicitly assumed that the initial pressure p_o is large enough that the absolute fluid pressure is always positive. Nonetheless, the predicted fluid pressure drop implies that cavitation could in principle take place, although this phenomenon cannot be modelled within the confines of this model which is based on the assumption of fluid incompressibility.

Figure 4 indicates that the opening increases approximately linearly with time, beyond $\tau = 0.1$ once the fluid pressure is nearly uniform in the crack, see Fig. 3. Figure 4 also suggests that the early stage of the crack opening can be described in an approximate fashion by the propagation of an "opening" front. Note, however, that change in crack width occurs instantaneously all along the crack from the onset of pressurization. It is these "early" opening changes which, although minute, are causing the early pressure drop. This is illustrated by the isochrones of the elastically induced crack opening, $\Omega_e \equiv \Omega - \Omega_o$, profiles which are plotted in Fig. 7. This figure gives clear evidence that the crack is closing in the tip region at early time.

Isochrones of the fluid pressure field are shown in Figs 5 and 6. (Figure 5 shows a subset of the isochrones at early time, i.e., $\tau < 0.05$.) Note that the time corresponding to each isochrone is indirectly given by the intercept $\gamma\tau$ of the isochrone with the pressure axis (here $\gamma = 4$). The early time pressure profiles are characterized by a minimum, which implies that fluid is flowing back from the tip region. The isochrones of $(p-p_o)/T$ for $\tau < \tau_1$ (where τ_1 is the time at which the fluid pressure at the tip reaches its minimum; here $\tau_1 \simeq 0.06$) appears to define an envelope, see Fig. 6. It is remarkable to observe that the pressure distribution is quasi-linear for $\tau > \tau_1$ (despite the strong non-linearity of the governing equations) and that the overall pressure gradient steadily decreases from that time on. At $\tau \simeq 0.15$, the crack is virtually uniformly pressurized with the pressure equal to its value on the boundary.

Finally, the evolution of the pressure gradient at the crack type, $\partial\Pi/\partial\xi = T^{-1}\partial p/\partial\xi$, is plotted in Fig. 8: the solid line curve corresponds to the finite difference approximation of the pressure gradient according to (B.10) in Appendix B, while the curve in dashed line is computed from (29), using the approximation (B.9) to compute the dimensionless stress intensity factor $\langle\Pi\rangle$ and its time derivative.

Asymptotic behavior

First, it is convenient to introduce the function $g(\xi, \tau)$, which is defined through the relation

$$\Pi = \gamma\tau[1 + g(\xi, \tau)]. \tag{32}$$

In view of the boundary condition for Π at $\xi = 1$ and the recognition that the evolution of Π is governed by a diffusion-type equation (which implies that the rate of change of Π is initially zero for $0 < \xi \leqslant 1$), we have that

$$\lim_{\tau \to 0} g(\xi, \tau) = \begin{cases} 1 & \xi = 0 \\ -1 & 0 < \xi \leqslant 1. \end{cases} \tag{33}$$

Also, the large time limit of $g(\xi, \tau)$ is given by

$$\lim_{\tau\to\infty} g(\xi,\tau) = 1 \quad 0 \leqslant \xi \leqslant 1. \tag{34}$$

This limit can be deduced from the following simple considerations. Since the crack opening Ω is unbounded with time τ (because of the linear increase of pressure at the crack inlet), the "conductivity" Ω^3 in the lubrication eqn (26) is also unbounded and thus Π is expected to become equal to its boundary value.

The large time behavior of $g(\xi,\tau)$ is of particular interest, in order to determine how "fast" the net crack loading Π equilibrates along the crack to its boundary value $2\gamma\tau$. Motivated by the quasi-linear pressure distribution shown in Fig. 6 at large time, we approximate the net loading by

$$g(\xi,t) = 1-r(\tau)\xi, \quad \tau > \tau_1 \tag{35}$$

where $r(\tau) > 0$ and $\lim_{\tau\to\infty} r(\tau) = 0$. In Appendix C, it is shown that the linear pressure distribution (35) is a good approximation of the large time solution of eqns (26) and (27). Furthermore, it is shown that $r(\tau) \sim \gamma^{-3}\tau^{-4}$, meaning that the net crack loading tends to the uniform distribution $2\gamma\tau$ as fast as $\gamma^{-3}\tau^{-4}$ goes to zero with time τ.

CALCULATION OF THE BREAKDOWN PRESSURE

Time influence function for the stress intensity factor

In view of the representation (32) of Π, the dimensionless stress intensity factor $\langle\Pi\rangle$ and its rate of change can be expressed as

$$\langle\Pi\rangle = 2\gamma\tau\Phi(\tau), \quad \frac{d\langle\Pi\rangle}{d\tau} = 2\gamma\left[\Phi(\tau)+\tau\frac{d\Phi(\tau)}{d\tau}\right] \tag{36}$$

where the time influence function $\Phi(\tau)$ is given by

$$\Phi = \frac{1}{2}\langle 1+g\rangle = \frac{1}{\pi\chi}\int_0^1 \frac{[1+g(\xi,\tau)]f(\xi)}{\sqrt{1-\xi^2}}d\xi. \tag{37}$$

Note that the influence function $\Phi(\tau)$ depends only on the two parameters Ω_o and γ. Actually, in view of the previous considerations on the dependance of the solution on Ω_o, we can write that

$$\Phi(\tau;\gamma,\Omega_o) = \Phi'(\Omega_o^3\tau;\Omega_o^{-4}\gamma). \tag{38}$$

Also, noting the asymptotic limits (33) of the function $g(\xi,\tau)$, the bounds of $\Phi(\tau)$ are

$$\lim_{\tau\to 0}\Phi(\tau) = 0$$

$$\lim_{\tau\to\infty}\Phi(\tau) = 1. \tag{39}$$

Note that $\Phi(0) = 0$ is a direct consequence of the fluid incompressibility assumption. (As a matter of fact, the value of $\Phi(0)$ characterizes the fluid pressure change in the crack under undrained conditions, i.e., under conditions when there is no change of fluid mass in the crack.) Note also that $\Phi(0) = 0$ implies that $d\langle\Pi\rangle/d\tau = 0$ at $\tau = 0$, see (36).

Asymptotic behaviors of the stress intensity factor are trivially deduced from (36) and (39). Note in particular that both $\langle\Pi\rangle$ and its rate of change vanish at $\tau = 0$. Plots of $\Phi(\tau)$ and $\langle\Pi\rangle(\tau)$ are shown in Fig. 9 (case $\Omega_o = 2$ and $\gamma = 4$). As expected from the known behavior of g, neither functions evolves monotonically with time.

Condition for breakdown

The condition of propagation of the edge crack (i.e., "breakdown") is given by

$$\langle \Pi \rangle(\tau_*) = 1 \tag{40}$$

where τ_* is the time at which breakdown occurs. From (36) and (40), we deduce the implicit equation

$$2\gamma\tau_*\Phi(\tau_*\,;\Omega_o,\gamma) = 2\gamma\tau_*\Phi'(\Omega_o^3\tau_*\,;\Omega_o^{-4}\gamma) = 1 \tag{41}$$

which can be solved to determine the dependence of the time to failure τ_* upon γ

$$\tau_* = \tau_*(\gamma\,;\Omega_o). \tag{42}$$

The above expression combined with

$$p_b - p_o = \gamma\tau_* T \tag{43}$$

yields the dependance of the breakdown pressure p_b on the rate of pressurization γ

$$p_b - p_o = h(\gamma\,;\Omega_o)T. \tag{44}$$

From the bounds of the function $\Phi(\tau)$, i.e., $\Phi(0) = 0$ and $\Phi(\infty) = 1$, it can readily be deduced that

$$\lim_{\gamma\to 0} h(\gamma) = \frac{1}{2} \tag{45}$$

$$\lim_{\gamma\to\infty} h(\gamma) = \infty. \tag{46}$$

It follows from (45) and (46) that a slow limit of the breakdown pressure exists, but that a fast limit cannot be identified.

Consider first the slow regime ($\gamma \to 0$). In this regime, the fluid pressure in the crack is virtually equilibrated with the pressure in the borehole at breakdown. From (44) and (45), the lower bound of the breakdown pressure p_b^l is given by

$$p_b^l \equiv p_o + T/2. \tag{47}$$

This limit actually corresponds to the breakdown criterion proposed by Haimson and Fairhurst (Haimson and Fairhurst (1967)). Note that the slow pressurization regime is practically reached at pressurization rates $\gamma < \gamma_l$, where the lower bound γ_l is arbitrarily defined from

$$p_b(\gamma_l) - p_b^l \simeq \delta(p_b^l - p_o) \tag{48}$$

with the relative error δ taken as 1%.

Consider next the fast regime ($\gamma \to \infty$). A fast limit cannot be identified as the breakdown pressure becomes unbounded with increasing pressurization rate. The non-existence of a finite bound on the breakdown pressure at large pressurization rates is a direct consequence of the assumption of fluid incompressibility. Indeed, the incompressibility assumption implies that $\Phi(0) = 0$, with the consequence that $h(\infty) = \infty$. In other words, the assumption of fluid incompressibility entails that the fluid pressure inside the crack can drop to arbitrarily large negative values with increasing pressurization rate, with the consequence that the breakdown pressure becomes unbounded with increasing γ. Obviously,

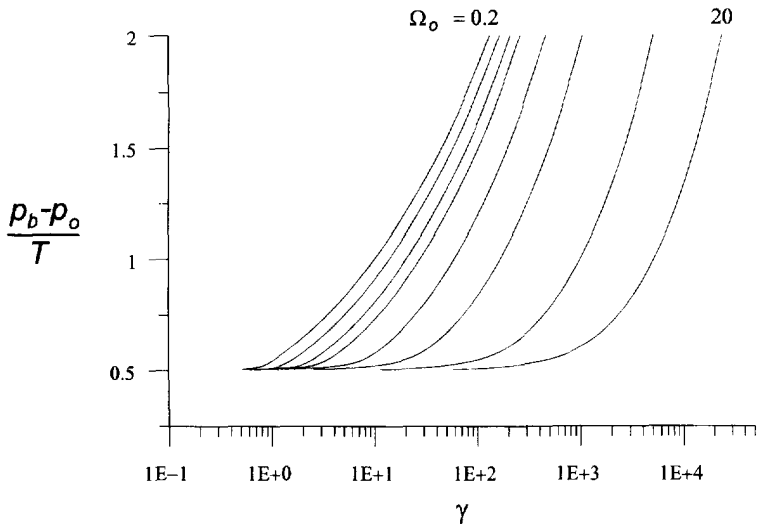

Fig. 10. Dimensionless breakdown pressure vs pressurization rate.

this predicted negative fluid pressure is physically meaningless since fluid can barely sustain any tension. In reality, cavitation would take place and for the fast pressurization regime we expect the crack to be totally cavitated (i.e., $p = 0$); hence $\langle \Pi \rangle \simeq \gamma\tau_* - p_o/T$ and, consequently, from (43)

$$p_b^u \equiv 2p_o + T \tag{49}$$

where p_b^u denotes the true upper bound of the breakdown pressure.

It is important to note that the Hubbert and Willis (1957) breakdown criterion $p_b - p_o \simeq T$ cannot really be justified within the framework of this model. Recall that this criterion is based on the assumption that the fluid pressure in the crack is still at its initial value p_o at breakdown. Since the fluid pressure can drop below its initial value p_o, it is clear that p_o does not correspond to the asymptotic value of the fluid pressure in the fast pressurization regime. Thus, the Hubbert-Willis limit cannot be considered as an upper bound of the breakdown pressure when the rock is impermeable (Haimson (1978)).

Variation of the normalized breakdown pressure with pressurization rate γ for Ω_o varying between 0.2 and 20 is shown in Fig. 10. As was already pointed out, the curves show that the breakdown pressure is characterized by a lower limit for the slow pressurization rate but is unbounded with increasing pressurization rates. Hence, there is no finite upper limit for the pressurization rate for the incompressible fluid model. However, we can establish a pseudo upper limit γ_u, by simply determining from these curves the pressurization rate corresponding to the true upper bound of the breakdown pressure p_b^u, which arises from consideration of cavitation in the crack. Correct determination of γ_u would require, however, consideration of fluid compressibility and cavitation.

For the pressurization rates γ between the threshold values for slow and fast regime, $\gamma_l < \gamma < \gamma_u$, the process is in the transient regime, with p_b depending on the pressurization rate A and varying from p_b^l to p_b^u as γ increases from γ_l to γ_u.

The lower and pseudo-upper limits of pressurization rate (γ_l, γ_u) are plotted vs the dimensionless initial opening Ω_o in Fig. 11 (γ_u is here calculated for $p_o = 0$). The graph shows that the pressurization limits grow monotonically with Ω_o, while tending to finite non-zero limits when Ω_o approaches zero: approximately $\gamma_l \to 0.4$ and $\gamma_u \to 8$ when $\Omega_o \to 0$. It also readily seen from Fig. 11 that the ratio γ_u/γ_l increases slightly from 20 to 10^2 with Ω_o in the interval $(0, 20)$.

CONCLUSIONS

In this paper a mathematical model is proposed to account for the influence of pressurization rate on the breakdown pressure. This model is based on the recognition that

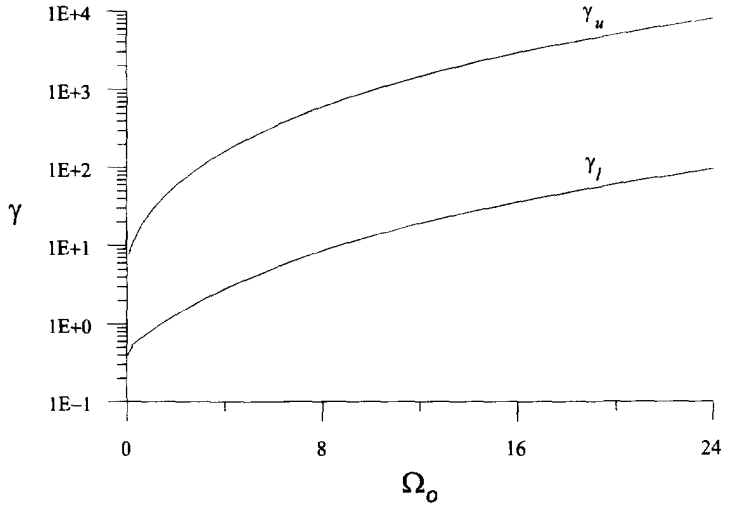

Fig. 11. Upper and lower limit of the pressurization rate vs dimensionless initial opening at the crack inlet. (Upper limit corresponds to $p_o = 0$.)

breakdown is associated with propagation of preexisting micro-cracks at the boundary of the borehole. Fluid flow in the crack is governed by a one-dimensional lubrication equation and is coupled with the non-local elastic response of the crack. Determination of the evolution of the fluid pressure and crack width lead to unexpected results: one is the drop of fluid pressure taking place at early times, which for "fast" pressurization rates can lead to cavitation in the crack; another is the occurrence of a local back flow in the crack.

Two key dimensionless parameters have been shown to control the magnitude of the breakdown pressure p_b: a dimensionless pressurization rate γ and a dimensionless initial crack opening Ω_o. A lower limit for the breakdown pressure (consistent with the Haimson-Fairhurst breakdown criterion) exists in the limit of slow pressurization rate. The corresponding lower limit γ_l depends only on Ω_o. An upper limit for p_b does not strictly exist within the framework of this model, which is based on the assumption of fluid incompressibility. Indeed, the fluid pressure in the crack can drop to arbitrarily large negative values with increasing pressurization rates. However, an upper bound can be determined by simply recognizing that a physically meaningful limit corresponds to the case where the crack is completely cavitated at breakdown—i.e., that the fluid pressure in the crack is everywhere equal to zero. The upper limit of pressurization rate γ_u depends on both Ω_o and p_o/T. This bound γ_u increases with p_o/T and consequently the range of pressurization rate $\gamma \in (\gamma_l, \gamma_u(p_o/T))$ for which the process is in transient regime is stretching in the direction of larger values of γ while its lower bound remains constant with increasing p_o.

Although the actual values for the bounds of the pressurization rate A depend on the parameters of the problem, the ratio $A_u/A_l = \gamma_u/\gamma_l$ depends formally only on the dimensionless initial opening of the crack Ω_o and on p_o/T. As can be seen from Fig. 11 (computed for the case $p_o = 0$), the ratio varies slightly with Ω_o and is of the order of 10^2 for the considered range of Ω_o, which corresponds to the typical range of variation of the parameters describing this problem. This ratio is three orders of magnitude lower than the one predicted in a previous study (Detournay and Cheng (1992)) and is in agreement with experimental results (Haimson and Zhao (1991), Schmitt and Zoback (1992), (1993)).

As a final note, it must be emphasized that the incompressible fluid model strictly applies when the fluid pressure is positive. This restriction actually implies that the model is applicable over a range of pressurization rates $[\gamma_l, \gamma_*]$, where γ_* is an increasing function of p_o/T.

Acknowledgments—Funding for the research reported in this paper has been partially provided by AECL, Canada which is gratefully acknowledged. The authors would also like to thank Dr Neil Chandler for his support.

REFERENCES

Bueckner, H. F. (1970). A novel principle for the computation of stress intensity factors. *ZAMP* **50,** 529–546.
Cundall, P. A. (1991). Improved fluid flow logic for udec. *Technical report*, Itasca Consulting Group, Minneapolis.
Detournay, E. and Carbonell, R. (1994). Fracture mechanics analysis of the breakdown process in mini-frac or leak-off test. In *Proc. EuRock'94, SPE/ISRM Rock Mechanics in Petroleum Engineering*, Balkema, Rotterdam, pp. 399–407.
Detournay, E. and Cheng, A. H.-D. (1992). Influence of pressurization rate on the magnitude of the breakdown pressure. In *Proceedings of 33rd U.S. Rock Mechanics Symposium*, Balkema, Rotterdam, pp. 325–333.
Haimson, B. and Fairhurst, C. (1967). Initiation and extension of hydraulic fractures in rocks. *Soc. Pet. Engng J.* **December,** 310–318.
Haimson, B. C. (1978). The hydrofracturing stress measuring method and recent field results. *International Journal of Rock Mechanics, Mining Science and Geomechanics Abstracts* **15,** 167–178.
Haimson, B. and Zhao, Z. Effect of borehole size and pressurization rate on hydraulic fracturing breakdown pressure. In *Proceedings of 32nd U.S. Symposium on Rock Mechanics*, Balkema, Rotterdam, pp. 191–199.
Hubbert, M. K. and Willis, D. G. (1957). Mechanics of hydraulic fracturing. *Transactions of the American Institute of Mining Engineers* **210,** 153–168.
Liskovets, O. A. (1965). The method of lines. *Journal of Differential Equations* **1,** 1308.
Nilson, R. H. and Proffer, W. J. (1984). Engineering formulas for fractures emanating from cylindrical and spherical holes. *ASME Journal of Applied Mechanics* **51,** 929–933.
Nilson, R. and Griffiths, S. (1983). Numerical analysis of hydraulically-driven fractures. *Computer Methods in Applied Mechanical Engineering* **36,** 359–370.
Paris, P. C., McMeeking, R. M., and Tada, H. (1976). The weight function method for determining the stress intensity factors. In *Cracks and Fractures* (eds Swedlow, J. L. and Williams, M. L.), pp. 471–489, ASTM Special Technical Publication 601, Philadelphia.
Pine, R. J. (1986). Rock joint and rock mass behaviour during pressurized hydraulic injections. PhD thesis, Camborne School of Mines, Cornwall, UK.
Rice, J. R. (1972). Some remarks on elastic crack-tip stress fields. *International Journal of Solids and Structures* **8,** 751–758.
Rice, J. (1968). *Fracture—An Advance Treatise*, volume II, Academic Press, New York.
Schmitt, D. R. and Zoback, M. D. (1992). Diminished pore pressure in low-porosity crystalline rock under tensional failure: apparent strengthening by dilatancy. *Journal of Geophysical Research* **97,** 273–288.
Schmitt, D. and Zoback, M. (1993). Infiltration effects in the tensile rupture of thin walled cylinders of glass and granite: Implications for the hydraulic fracturing breakdown equation. *International Journal of Rock Mechanics, Mining Science and Geomechanics Abstracts* **30,** 289–303.
Shapiro, R. A. (1954). *The Dynamics and Thermodynamics of Compressible Fluid Flow*, volume II, Ronald Press, New York.
W. H. Press, S. A., Teukolsky, W. V. and Flannery, B. (1992). *Numerical Recipes*, 2nd edition, Cambridge University Press, UK.

APPENDIX A: IRRELEVANCE OF FLUID COMPRESSIBILITY

In this appendix we demonstrate that fluid compressibility can be neglected. Consider the lubrication equation for compressible fluid

$$\frac{\partial \rho\Omega}{\partial \tau} = \frac{\partial}{\partial \xi}\left(\rho\Omega^3 \frac{\partial \Pi}{\partial \xi}\right) \tag{A.1}$$

where the fluid density ρ is a function of the fluid pressure p. Now expand the time derivative of $\rho\Omega$

$$\frac{\partial \rho\Omega}{\partial \tau} = \Omega \frac{\partial \rho}{\partial \tau} + \rho \frac{\partial \Omega}{\partial \tau}. \tag{A.2}$$

Fluid compressibility effects are negligible if

$$\alpha \equiv \frac{\Omega\left|\dfrac{\partial \rho}{\partial \tau}\right|}{\rho\left|\dfrac{\partial \Omega}{\partial \tau}\right|} \ll 1. \tag{A.3}$$

An estimate of α can be obtained as follows. First note that the fluid pressure is much smaller than the fluid bulk modulus K_f, since $p = O(T)$ at most with $T \sim 10$ MPa and $K_f \sim 10^4$ MPa. Hence, a linear dependance of ρ on p can be assumed, i.e.,

$$\rho = \rho_o\left(1 + \frac{p}{K_f}\right). \tag{A.4}$$

The time derivative of the fluid density can then be written as

$$\frac{\partial \rho}{\partial \tau} = \frac{\rho_o}{K_f}\frac{\partial p}{\partial \tau} = \rho_o \frac{T}{K_f}\left(\frac{\partial \Pi}{\partial \tau} - \gamma\right)$$

where the definition of Π and $\partial\sigma/\partial\tau = -\gamma$ have been used. Taking the following estimates: $|\partial\Omega/\partial\tau| \sim \gamma$, $|\partial\Pi/\partial\tau| \sim 2\gamma$, $\rho \sim \rho_o$, and $\Omega \sim \Omega_o + 1$ (which corresponds to the opening at breakdown) we find that

$$\alpha \sim (\Omega_o + 1)\frac{T}{K_f}. \tag{A.5}$$

Since $E' \sim 10^4$ MPa, $w_o/\lambda \sim 10^{-3} \div 10^{-2}$ ($\lambda \sim 1 \div 10$ mm), $\Omega_o \sim 10^{-2} \div 10$, we find that $\alpha = O(10^{-2})$ at most. The number α is then typically a small number and therefore fluid compressibility effects are negligible, according to (A.3).

APPENDIX B: NUMERICAL PROCEDURE

A general method-of-lines numerical approach (Liskovets (1965), Nilson and Griffiths (1983)) is used to solve the system of coupled eqns (26) and (27) for the pressure $\Pi(\xi, \tau)$ and the crack opening $\Omega(\xi, \tau)$ for a prescribed pressure at the crack inlet $\Pi(0, \tau)$ and a no-flow condition at the crack tip. The numerical algorithm is outlined below.

Principle of the general method-of-lines

The method-of-lines can be applied to solve systems of differential, integral or integro-differential equations in some given domain $D^{(n)}$ in an n-dimensional space, $n \geqslant 2$. The essence of the method is to discretize the unknown functions in an r-dimensional subset of $D^{(n)}$ (and not in the original n-dimensional space of the problem, as in conventional finite difference numerical schemes), while the functions are taken to vary continuously in the complementary $(n-r)$-dimensional space (Liskovets (1965)). The initial system of equations on $D^{(n)}$ is then reduced to a system of equations on a certain domain $D^{(n-r)}$ of lower dimension, provided that the boundary conditions for the initial system, given on $\partial D^{(n)}$, can be appropriately transferred into the boundary conditions on $\partial D^{(n-r)}$. If $r = n-1$, the initial system is reduced to a system of ordinary differential equations (or mixed system of ordinary differential and integral equations on $D^{(1)}$). If $r = n$ the initial system is transformed into a system of equations on $D^{(0)}$ or, in other words, to a system of algebraic equations (as in conventional finite differences schemes).

Numerical algorithm

The algorithm relies on the so-called "longitudinal" scheme in which the discretization is performed with respect to the spatial coordinate ξ and a solution varying continuously in time τ is sought. (In the "transverse" scheme, time is discretized and the solution is continuous in the space coordinates.)

First, a set of equally spaced fixed grid points $\{\xi_i\}$, $i = 1, \ldots, M$ with $\xi_1 = 0$ and $\xi_M = 1$ is selected. The dimensionless net pressure Π is then approximated with order of error $O(\Delta\xi^2)$ ($\Delta\xi$ denoting the grid step) by a piecewise linear function defined by it values $\{\Pi_i(\tau)\}$ at grid points $\{\xi_i\}$

$$\Pi(\xi, \tau) = \Pi_i + \frac{\Pi_{i+1} - \Pi_i}{\xi_{i+1} - \xi_i}(\xi - \xi_i), \quad \xi \in [\xi_i, \xi_{i+1}). \tag{B.1}$$

Next the dimensionless crack opening Ω, corresponding to the piecewise linear net pressure distribution (B.1), can be computed according to (27)

$$\Omega(\xi, \tau) = \Omega_0(\xi) + \sum_{i=1}^{M} \Xi_i(\xi)\Pi_i(\tau). \tag{B.2}$$

The influence coefficients Ξ_i for a constant grid step $\xi_{i+1} - \xi_i = \Delta\xi$, $\forall i$ are given by the following formulae

$$\Xi_1(\xi) = \left[G_3(\eta) - \frac{1}{\Delta\xi}G_4(\eta) - \left(G_1(\eta, \xi_1) - \frac{1}{\Delta\xi}G_2(\eta, \xi_1)\right)\right]_{\min(\xi,\xi_2)}^{\xi_2}$$
$$+ \left[\left[G_1(\eta, \zeta) - \frac{1}{\Delta\xi}G_2(\eta, \zeta)\right]_{\zeta=\xi_1}^{\zeta=\xi_2}\right]_{\max(\xi,\xi_2)}^{1},$$

$$\Xi_2(\xi) = \frac{1}{\Delta\xi}[G_4(\eta) - G_2(\eta, \xi_1)]_{\min(\xi,\xi_2)}^{\xi_2}$$
$$+ \left[\frac{1}{\Delta\xi}[G_2(\eta, \zeta)]_{\xi_1}^{\xi_2} + 2(G_3(\eta) - G_1(\eta, \xi_2)) - \frac{1}{\Delta\xi}(G_4(\eta) - G_2(\eta, \xi_2))\right]_{\max(\xi,\xi_2)}^{\max(\xi,\xi_3)}$$
$$+ \left[\left[2G_1(\eta, \zeta) - \frac{1}{\Delta\xi}G_2(\eta, \zeta)\right]_{\zeta=\xi_2}^{\zeta=\xi_3} + \frac{1}{\Delta\xi}[G_2(\eta, \zeta)]_{\xi_1}^{\xi_2}\right]_{\max(\xi,\xi_3)}^{1},$$

$$\Xi_i(\xi) = \Phi_i^1(\xi) + \Phi_i^2(\xi) + \left[\left[iG_1(\eta,\zeta) - \frac{1}{\Delta\xi} G_2(\eta,\zeta) \right]_{\zeta=\xi_i}^{\zeta=\xi_{i+1}} + \left[-(i-2)G_1(\eta,\zeta) + \frac{1}{\Delta\xi} G_2(\eta,\zeta) \right]_{\xi_{i-1}}^{\xi_i} \right]_{\max(\xi,\xi_{i-1})}^{1}, \tag{B.3}$$

for $3 \leqslant i \leqslant M-2$

$$\Xi_{M-1}(\xi) = \Phi_{M-1}^1(\xi) + \Phi_{M-1}^2(\xi), \quad \Xi_M(\xi) = \Phi_M^1(\xi).$$

The functions appearing above are defined as

$$\Phi_i^1(\xi) \equiv \left[-(i-2)(G_3(\eta) - G_1(\eta,\xi_{i-1})) + \frac{1}{\Delta\xi}(G_4(\eta) - G_2(\eta,\xi_{i-1})) \right]_{\max(\xi,\xi_{i-1})}^{\max(\xi,\xi_i)}$$

$$\Phi_i^2(\xi) \equiv \left[\left[-(i-2)G_1(\eta,\zeta) + \frac{1}{\Delta\xi} G_2(\eta,\zeta) \right]_{\zeta=\xi_{i-1}}^{\zeta=\xi_i} + i(G_3(\eta) - G_1(\eta,\xi_i)) + \frac{1}{\Delta\xi}(G_2(\eta,\xi_i) - G_4(\eta)) \right]_{\max(\xi,\xi_i)}^{\max(\xi,\xi_{i+1})}$$

$$G_\alpha(\eta,\zeta;\xi) \equiv \frac{8}{\pi}\int^\eta I_\alpha(\eta,\zeta)\frac{f(\xi/\eta)\eta\,\mathrm{d}\eta}{\sqrt{\eta^2-\xi^2}}, \quad G_{2+\alpha}(\eta;\xi) \equiv \frac{8}{\pi}\int^\eta I_\alpha(\eta,\eta)\frac{f(\xi/\eta)\eta\,\mathrm{d}\eta}{\sqrt{\eta^2-\xi^2}}, \quad \alpha = 1,2$$

$$I_\alpha(\eta,\zeta) \equiv \int_0^\zeta \frac{\zeta^{\alpha-1} f(\zeta/\eta)\,\mathrm{d}\zeta}{\sqrt{\eta^2-\zeta^2}}, \quad \alpha = 1,2$$

where we use the convention that

$$[g(\eta,\zeta)]_c^d \equiv g(\eta,d) - g(\eta,c), \quad [h(\eta)]_a^b \equiv h(b) - h(a), \quad \forall g(\cdot,\cdot), h(\cdot).$$

The integrals $I_\alpha(\eta,\zeta)$ and $G_{2+\alpha}(\eta;\xi)$ can be solved analytically; their close form expressions are given below

$$I_1(\eta,\zeta) = \chi_1 \arcsin\left(\frac{\zeta}{\eta}\right) + \chi_2\sqrt{1-\left(\frac{\zeta}{\eta}\right)^2}$$

$$I_2(\eta,\zeta) = \eta\left\{-\chi_1\sqrt{1-\left(\frac{\zeta}{\eta}\right)^2} - \frac{\chi_2}{2}\left(\arcsin\left(\frac{\zeta}{\eta}\right) - \frac{\zeta}{\eta}\sqrt{1-\left(\frac{\zeta}{\eta}\right)^2}\right)\right\}$$

$$G_3(\eta;\xi) = 4\chi_1\{\chi_1\sqrt{\eta^2-\xi^2} - \chi_2\xi\ln(\eta+\sqrt{\eta^2-\xi^2})\}$$

$$G_4(\eta;\xi) = -2\chi_2\left\{\left(-\chi_2\xi + \frac{\chi_1\eta}{2}\right)\sqrt{\eta^2-\xi^2} + \frac{1}{2}\chi_1\xi^2\ln(\eta+\sqrt{\eta^2-\xi^2})\right\}.$$

However $G_\alpha(\eta,\zeta;\xi)$, $\alpha = 1,2$ cannot be evaluated in terms of elementary functions and needs to be calculated numerically for each combination of the arguments.

The lubrication eqn (26) can be integrated with respect to ξ from $\xi_{j-1/2}$ to $\xi_{j-1/2}$ for j taking values from 2 to $M-1$ and from $\xi_{M-1/2}$ to $\xi_M = 1$ to yield

$$\sum_{i=1}^{M} \Theta_{ji}\dot{\Pi}_i + O(\Delta\xi^2) = \Delta Q_j, \quad j = 2,\ldots,M-1 \tag{B.4}$$

$$\sum_{i=1}^{M} \Theta_{Mi}\dot{\Pi}_i + O(\Delta\xi^2) = \Delta Q_M, \tag{B.5}$$

where

$$\Delta Q_j \equiv Q_{j-1/2} - Q_{j+1/2}, \quad \Delta Q_M \equiv Q_{M-1/2} - Q_M,$$

$$\Theta_{ji} \equiv \int_{\xi_{j-1/2}}^{\xi_{j-1/2}} \Xi_i(\xi)\,\mathrm{d}\xi = \Xi_{ji}\Delta\xi + O(\Delta\xi^2), \quad j = 2,\ldots,M-1,$$

$$\Theta_{Mi} \equiv \int_{\xi_{M-1/2}}^{1} \Xi_i(\xi)\,\mathrm{d}\xi = \Xi_{M-1/4i}\frac{\Delta\xi}{2} + O(\Delta\xi^2), \quad \Xi_{xi} \equiv \Xi_i(\xi_x).$$

The right-hand sides of equations (B.4) and (B.5) are approximated to $\Delta\xi^2$ as follows

$$\Delta Q_j = \Omega^3_{j+1/2}\frac{\Pi_{j+1}-\Pi_j}{\Delta\xi} - \Omega^3_{j-1/2}\frac{\Pi_j-\Pi_{j-1}}{\Delta\xi} + O(\Delta\xi^2) \tag{B.6}$$

$$\Delta Q_M = -\Omega^3_{M-1/2}\frac{\Pi_M-\Pi_{M-1}}{\Delta\xi} + O(\Delta\xi^2) \tag{B.7}$$

with

$$\Omega^3_{j-1/2} \equiv \frac{\Omega^3_j + \Omega^3_{j-1}}{2}.$$

Note that the zero-flow boundary condition at the tip of the crack, $Q_M = 0$, was utilized to obtain (B.7).

Substitution of (B.6) and (B.7) into eqns (B.4) and (B.5) together with the initial condition and the boundary condition at the crack inlet, (28), yields a system of ordinary differential equations in time with unknowns Π_i, $i = 2, \ldots, M$

$$\Delta\xi^2 \sum_{i=1}^{M} \Xi_{ji}\dot{\Pi}_i = \Omega^3_{j+1/2}(\Pi_{j+1}-\Pi_j) - \Omega^3_{j-1/2}(\Pi_j-\Pi_{j-1}), \quad j = 2, \ldots, M-1,$$

$$\frac{1}{2}\Delta\xi^2 \sum_{i=1}^{M} \Xi_{M-1,i}\dot{\Pi}_i = -\Omega^3_{M-1/2}(\Pi_M-\Pi_{M-1}), \tag{B.8}$$

with

$$\Pi_j(\tau = 0) = 0, \quad j = 1, \ldots, M \quad \text{and} \quad \Pi_1(\tau) = 2\gamma\tau.$$

The system of ordinary coupled differential equations (B.8) is solved numerically by means of a modified Runge-Kutta 5th order numerical scheme with adaptive time step to preserve desired accuracy (Press *et al.* (1992)).

Calculation of the breakdown condition

In order to monitor the breakdown condition (40), $\langle\Pi\rangle(\tau_*) = 1$, the stress intensity factor has to be evaluated numerically. We use the piecewise linear distribution (B.1) for the net pressure to obtain an approximation for the dimensionless stress intensity factor $\langle\Pi\rangle$, which is calculated by integrating exactly (30)

$$\langle\Pi\rangle(\tau) = \frac{2}{\chi\pi}\sum_{i=1}^{M-1}[a_i^1 Y_1(\xi) + a_i^2 Y_2(\xi) + a_i^3 Y_3(\xi)]_{\xi=\xi_i}^{\xi=\xi_{i+1}} + O(\Delta\xi^2) \tag{B.9}$$

where

$$a_i^1 = \chi_1(\Pi_i - (i-1)(\Pi_{i+1}-\Pi_i)),$$

$$a_i^2 = \frac{\chi_1}{\Delta\xi}(\Pi_{i+1}-\Pi_i) - \chi_2(\Pi_i - (i-1)(\Pi_{i+1}-\Pi_i)),$$

$$a_i^3 = -\frac{\chi_2}{\Delta\xi}(\Pi_{i+1}-\Pi_i),$$

and

$$Y_1(\xi) = \arcsin(\xi), \quad Y_2(\xi) = -\sqrt{1-\xi^2}, \quad Y_3(\xi) = \tfrac{1}{2}(Y_1(\xi) + \xi Y_2(\xi)).$$

Note that the solution of (B.8) can be checked by comparing the analytically estimated value of pressure gradient at the tip of the crack (29) (which requires calculating the stress intensity factor and its time derivative at each time step using (B.9)) with the finite difference approximation

$$\left.\frac{\partial\Pi}{\partial\xi}\right|_{\xi=1} = \frac{1}{2\Delta\xi}[3\Pi_M - 4\Pi_{M-1} + \Pi_{M-2}] + O(\Delta\xi^2) \tag{B.10}$$

APPENDIX C: ASYMPTOTICS CALCULATION

We seek to determine whether the linear pressure distribution assumed for large time, see (35), is consistent with (26) and (27), and also how "fast" the pressure distribution along the crack tends towards the uniform value $2\gamma\tau$. The crack opening corresponding to a linear net pressure distribution, given by (32) and (35), can be deduced from (27) to be

$$\Omega = \Omega_o\sqrt{1-\xi^2} + \gamma\tau[2\omega_o(\xi) - r(\tau)\omega_1(\xi)] \tag{C.1}$$

where the function $\omega_o(\xi)$ is given by

$$\omega_o(\xi) \equiv 4\left(\chi_1 - 2\frac{\chi_2}{\pi}\right)\left(\chi_1\sqrt{1-\xi^2} + \chi_2\,\xi \ln\left(\frac{\xi}{1+\sqrt{1-\xi^2}}\right)\right). \tag{C.2}$$

(An expression for $\omega_1(\xi)$—the elastically induced crack opening due to linear pressure distribution along the crack—could also be derived, but for the following considerations it is only of interest to know that this function is bounded.) Substituting (32) with (35) and (C.1) into the lubrication eqn (26) and dropping the terms of order τ^α, $\alpha < 0$ (assuming that $r(\tau) \sim \tau^\beta$, $\beta < -1$) leads to

$$-\frac{\omega_o(\xi)}{8\gamma^3(\omega_o^3(\xi))'} = \tau^4 r(\tau) \tag{C.3}$$

where $'$ here denotes the derivative with respect to ξ. The relation (C.3) requires that

$$r(\tau) = A\tau^{-4}. \tag{C.4}$$

Solving the differential equation (C.3) for ω_o yields

$$\omega_o(\xi) = \sqrt{\frac{1-\xi}{12\gamma^3 A}}. \tag{C.5}$$

Comparison of the expression (C.5) for $\omega_o(\xi)$, obtained through the lubrication equation, with (C.2), calculated directly by integration of (27), shows that the two expressions give virtually the same crack opening, provided that

$$A \simeq (5.7\sqrt{12})^{-2}\gamma^{-3} = 0.00256\gamma^{-3}. \tag{C.6}$$

So, indeed, the net crack loading Π can be approximated by a linear function (35) for large times. Furthermore, Π tends to the uniform distribution $2\gamma\tau$ as fast as $\gamma^{-3}\tau^{-4}$ goes to zero when $\tau \to \infty$.